Available online at www.sciencedirect.com
ScienceDirect
Journal of Physics and Chemistry of Solids 68 (2007) 1147–1151
JOURNAL OF PHYSICS AND CHEMISTRY OF SOLIDS
www.elsevier.com/locate/jpcs

Preparation and structural investigations of sol–gel derived Eu^{3+}-doped $CaAl_2O_4$

Stanislava Janáková[a,*], Linda Salavcová[a], Guillaume Renaudin[b], Yaroslav Filinchuk[c], Damien Boyer[b], Philippe Boutinaud[b]

[a]Department of Inorganic Chemistry, Institute of Chemical Technology, Technicka 5, 166 28 Prague, Czech Republic
[b]Laboratoire des Matériaux Inorganiques, UMR CNRS 6002, Université Blaise Pascal et ENSCCF, 24 Avenue des Landais, F-63177 Aubière Cedex, France
[c]Swiss-Norwegian Beam Lines at ESRF, 6 rue Jules Horowitz, BP-220, 38043 Grenoble, France

Abstract

Monoclinic and hexagonal undoped and Eu^{3+}-doped calcium aluminates ($CaAl_2O_4$) were prepared as powders using sol–gel methodology after thermal treatments at 850 °C (hexagonal form) or 1200 °C (monoclinic form). Attempt was made to solve the unknown structure of the metastable hexagonal form by synchrotron powder diffraction in an average $P6_3$ model. The structural features of the metastable phase were investigated using infrared and Raman spectroscopies and by studying the luminescence properties of the Eu^{3+}doped phases.

Keywords: A. Inorganic compounds; A. Optical materials; D. Luminescence

1. Introduction

Divalent Europium doped $CaAl_2O_4$ (CA : Eu^{2+}; using the cement chemistry shorthand) is a well-known bluish-green emitting phosphor able to show bright afterglow under UV irradiation [1]. In the past years, efforts have been concentrated on the afterglow properties of the stable monoclinic form of CA : Eu^{2+} that can be readily prepared by solid state reaction at around 1300 °C in reducible atmosphere [2–4]. More recently, low temperature routes (Pechini combustion or sol–gel technology) have been experienced as relevant for the preparation of this phosphor as powders and films [5–7]. These methods also allowed stabilizing the metastable hexagonal form of CA after thermal treatment at 850 °C [6,7]. The hexagonal to monoclinic phase transition was reported at 950 °C [6]. As the crystal structure of the metastable CA form has not yet been solved, we decided to investigate the structural features of this phase by combining X-ray powder diffraction, vibrational spectroscopy and photoluminescence technique, using the Eu^{3+} ion as a local probe. In this paper, we present the preparation of monoclinic and hexagonal CA and CA : Eu^{3+} powders and preliminary structural investigations leading to an average hexagonal $P6_3$ model.

2. Experimental methods

CA and CA : Eu^{3+} (1%) were prepared by dissolving anhydrous $CaCl_2$ (and $EuCl_3$ in appropriate amount when required, Eu replacing Ca) and $Al(^iPrO)_3$ in anhydrous isopropanol. This solution was mixed to a solution containing metallic potassium dissolved in isopropanol at 85 °C in a dry argon atmosphere. A transparent sol was obtained after removal of KCl precipitates by centrifugation. This sol was hydrolyzed and condensed to a gel that was dried at 100 °C for 4 h to form a white xerogel. The metastable hexagonal form of CA and CA : Eu^{3+} powders were prepared by thermal treatment at 850 °C in air for 4 h. The high temperature monoclinic phase (undoped or doped) was obtained by heating at 1200 °C for 6 h. The X-ray powder diffraction patterns were recorded either at room temperature or *versus* temperature up to 1200 °C using a θ/θ Philips X'Pert diffractometer (Cu anode)

*Corresponding author. Tel.: +420 22044 4003; fax: +420 22044 4411.
E-mail addresses: stanislava.janakova@vscht.cz (S. Janáková), philippe.boutinaud@univ-bpclermont.fr (P. Boutinaud).

0022-3697/$ - see front matter © 2007 Elsevier Ltd. All rights reserved.
doi:10.1016/j.jpcs.2006.12.034

equipped with a high temperature attachment. We used a sequential temperature rising rate of 10 °C/min and a temperature holding time of 1 h before each measurement. Temperature was measured by means of Pt/Pt–Rd thermocouple in direct contact with the powder deposited on a Pt ribbon. A synchrotron powder diffraction pattern was collected at room temperature on the metastable undoped CA at the SNBL (BM1) at ESRF, Grenoble (six analyser crystals detector, $\lambda = 0.40008$ Å, 2θ range 2.53°−37.5°, two theta step 0.005°, sample in a glass capillary of 0.3 mm diameter). Infrared absorption spectra were measured on a Nicolet FTIR spectrophotometer in the range 400−4000 cm^{-1} using the KBr pellet technique. MicroRaman diffusion spectra were recorded at room temperature in the range 400−950 cm^{-1} using a Jobin Yvon T64000 spectrometer. Steady-state photoluminescence spectra were recorded at room temperature using a monochromatized xenon lamp as excitation source and a TRIAX 550 Jobin-Yvon/Horiba monochromator equipped with a photomultiplier as the detector. Site selective luminescence spectra were measured using a tunable ND60 dye laser operated with a mixture of rhodamines 590 + 610 pumped by a pulsed Continuum Surelite I SL-10 frequency doubled Nd:YAG laser. The output of the dye laser was frequency shifted by stimulated Raman effect using a H_2 Raman cell for an excitation in the blue spectral range. A liquid nitrogen-cooled home-made cold finger was used for low temperature measurements.

3. Results and discussion

3.1. Temperature dependence of the X-ray powder diffraction

The temperature dependence of the X-ray diffraction patterns of undoped and Europium-doped CA xerogels is presented in Fig. 1. The strong peaks at around $2\theta = 39°$ and $2\theta = 46°$ in Fig. 1(a) are due to the Pt ribbon and should not be considered for phase indexation. This is clear from the Figure that the undoped CA sample is amorphous up to 800 °C and crystallizes as the metastable hexagonal phase at 850 °C. This phase transforms to the stable monoclinic one at 1050 °C, as indicated by the splitting of the diffraction peak situated at around $2\theta = 35°$ (see arrow in Fig. 1a). Rietveld refinement of the powder pattern of the undoped sample recorded at 1200 °C was achieved using the program *FullProf* [8]. The result indicated a perfect agreement with the $P2_1/n$ monoclinic structure [9]. The Le Bail fit of the powder pattern of the undoped sample recorded at 900 °C converged to a hexagonal cell with $a = 8.7402(2)$ Å and $c = 8.0904(2)$ Å in agreement with Ref. [6] and corresponds also to the ortho-hexagonal lattice previously reported in Ref. [10]. Concerning Europium-doped CA, it is interesting to note that the temperature of first crystallization is up-shifted by 100 °C compared to the undoped sample. Within the experimental conditions we used, we note that the hexagonal phase is still present at 1200 °C. This latter phase was completely transformed to monoclinic CA : Eu^{3+} after thermal treatment at higher temperature or for longer periods-(typically 1150 °C for 8 h, 1200 °C for 6 h or 1300 °C for 4 h).

3.2. Refined metastable hexagonal model

Synchrotron powder diffraction pattern was collected on the metastable phase synthesized at 900 °C. The program *Expo2004* [11] was used to check the numerous trigonal and hexagonal space groups compatible with the extinction rules. The best solution was obtained with the space group $P6_3$ ($Z = 6$) with a R'_p value above 20% and without localization of the oxygen sites. Three calcium positions (one in site 2*a* and two in site 2*b*) and two aluminium positions (in general position 6*c*) have been found. Then, oxygen positions have been localized by global optimization in direct space with the program *Fox* [12] by defining rigid AlO_4 tetrahedra and optimizing their orientation while keeping other structural parameters fixed. A solution was rapidly obtained leading to four independent oxygen sites in general 6*c* position. Rietveld refinement of this

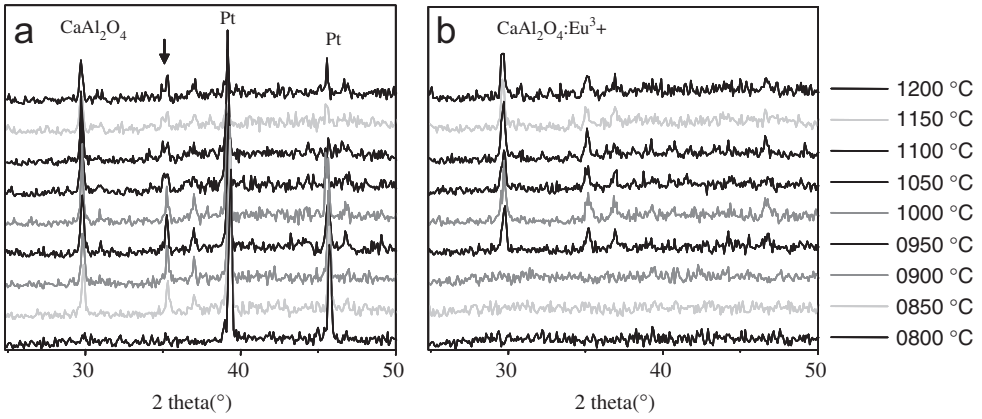

Fig. 1. Temperature dependence of X-ray diffraction patterns of CA (a) and CA : Eu^{3+} (b). The peaks of Pt ribbon have been removed from the patterns in (b).

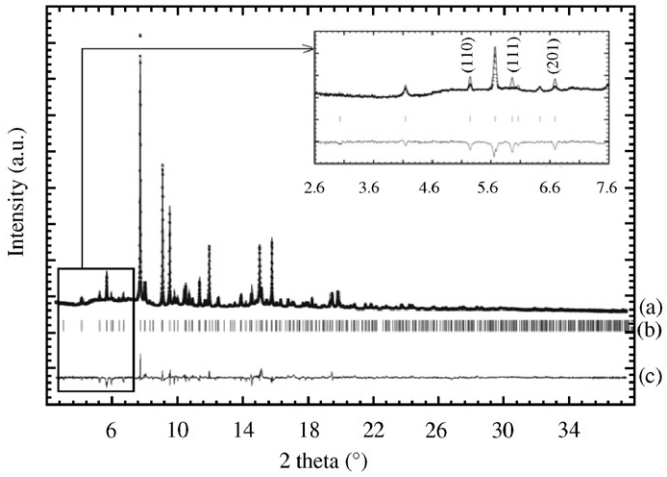

Fig. 2. Rietveld plot of hexagonal $P6_3$ metastable CA model: (a) observed (dots) and calculated (solid line) synchrotron (SNBL) powder diffraction patterns ($\lambda = 0.40008$ Å), (b) Bragg peaks positions and (c) difference curve.

Table 1
Atomic positional and displacement parameters for hexagonal $P6_3$ metastable CA.

	Site	x	y	z	B ($Å^2$)
Ca1	2*b*	2/3	1/3	0.2451 (9)	1.69 (6)
Ca2	2*b*	1/3	2/3	0.2974 (9)	= B(Ca1)
Ca3	2*a*	0	0	0.262 (1)	= B(Ca1)
Al1	6*c*	0.674 (2)	0.018 (2)	0.505 (1)	0.94(5)
Al2	6*c*	0.653 (1)	0.678 (1)	0.4546 (6)	= B(Al1)
O1	6*c*	0.5788 (9)	0.787 (1)	0.212 (2)	2.57 (8)
O2	6*c*	0.453 (2)	0.918 (1)	0.513 (2)	= B(O1)
O3	6*c*	0.769 (1)	0.880 (2)	0.545 (2)	= B(O1)
O4	6*c*	0.785 (3)	0.206 (3)	0.445 (3)	= B(O1)

hexagonal $P6_3$ model was performed using *FullProf* [8]. The results (see Fig. 2 and Table 1) indicated that the $P6_3$ structure description cannot be considered as a definitive model but only as an average one. Discrepancies from the refined $P6_3$ model are expressed by a high final χ^2 value of 11.6 ($R_p = 0.06$ and $R_{wp} = 0.09$, background corrected). This is illustrated in the insert in Fig. 2 showing the bad fitting of Bragg peaks (1 1 0), (1 1 1) and (2 0 1), mainly because of a bad localization of the O1 site leading to short Ca2–O1 distances and long Al1–O1 and Al2–O1 distances. Any attempt to solve the structure by lowering the symmetry (i.e. to orthorhombic) has not been successful.

3.3. Infrared and Raman spectra

Representative infrared absorption and micro-Raman diffusion spectra of undoped hexagonal and monoclinic CA samples are shown in Fig. 3. While the general features of the infrared spectra are similar for the two phases, significant differences are observed in the Raman spectra. The infrared spectra consist of four groups of signals: a broad band in the range 410−470 cm^{-1} (labelled as band A), two groups of doublets at, respectively, 530 – 570 and 630−730 cm^{-1} (labelled as bands B and C) and a band in the range 770−870 cm^{-1} (labelled as band D). Similitudes in infrared spectra agree with the similitudes in the tetrahedral AlO_4 network in the monoclinic and the average hexagonal structures. Concerning the Raman spectra, we note that the shoulder present at 545 cm^{-1} for monoclinic CA (see arrow in Fig. 3(b)) is not present in hexagonal CA and that a number of additional modes (or mode splitting) appears in the latter phase (see arrows in Fig. 3(b)). The band at 790 cm^{-1} is ascribed to Al–O stretching modes while the strong Raman band at 520 cm^{-1} and its shoulder at 545 cm^{-1} are related to motions of bridging oxygen atoms within the Al–O–Al linkages [13]. These observations can be attributed either to a change in the point group symmetry of AlO_4 (inconsistent with the average hexagonal model), or to a decrease of the number of independent Al crystallographic sites (consistent with the average hexagonal model).

3.4. Photoluminescence

Typical steady-state luminescence spectra of the two CA : Eu^{3+} phases are shown in Fig. 4. The Eu^{3+} emission consists of transitions between the excited $^5D_0$ level and the lower lying ^7F_J Stark components, with $J = 0, 1, 2, 3$ and 4 and is dominated by the hypersensitive electric dipole $^5D_0 \rightarrow {}^7F_2$ transition in both phases. Interestingly, we notice strong differences in the spectral features of the emission going from monoclinic to hexagonal CA : Eu^{3+}. Similarly, significant differences are observed in the excitation spectra since the spectrum of the hexagonal phase is dominated by the intraconfigurational $^7F_0 \rightarrow {}^5L_6$ transition peaking at around 395 nm, while the spectrum of the monoclinic phase is dominated by a strong UV band peaking at around 260 nm. Considering that the absorption edge of the CA host is at about 215 nm [14], the 260 nm band cannot result from host sensitization of the Eu^{3+} luminescence in CA. According to Dorenbos' model applied to the location of 4f–5d bands of rare-earth ions in inorganic media, it is possible to predict the energy of the lowest 4f–5d transition of Eu^{3+} ions in $CaAl_2O_4$ from the knowledge of the position of 4f–5d band of Ce^{3+} ions in the same host. The lowest 4f–5d transition of Ce^{3+} in $CaAl_2O_4$ (monoclinic form) is around 361 nm [14]. Using the Dorenbos' equation [15], the lowest 4f–5d transition of Eu^{3+} is predicted at about 157 nm, which is much higher in energy than the band observed at 260 nm. We therefore ascribe this latter band to $O^{2-} \rightarrow Eu^{3+}$ charge transfer. Site selective experiments were also carried out at 120 K on the hexagonal CA : Eu^{3+} phase. A selection of emission and excitation spectra is proposed in Fig. 5. The emission spectra were recorded upon various excitation wavelengths in either $^5D_0$ or $^5D_2$ multiplets. Despite the relatively low intensity of the signals it is clear that several optical signatures are evidenced, indicating that the Eu^{3+} ions

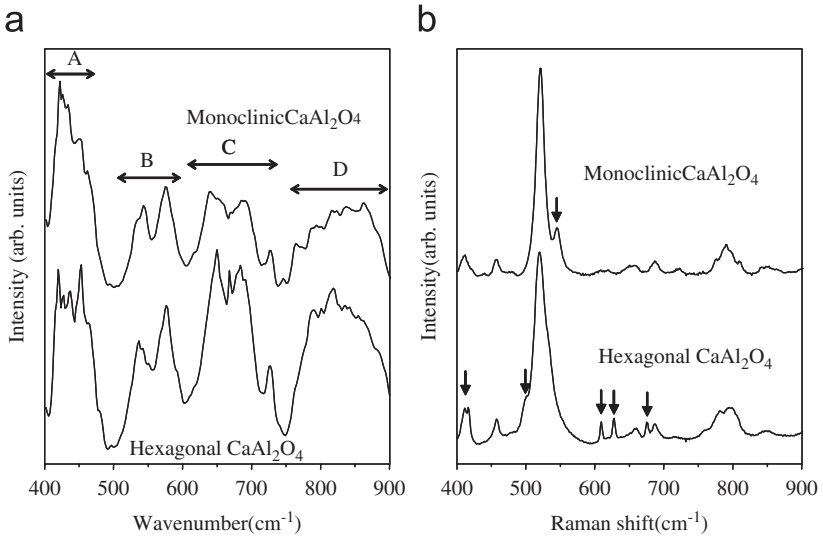

Fig. 3. Infrared absorption (a) and microRaman diffusion (b) spectra of monoclinic and hexagonal CA phases at room temperature. Symbols are defined in the text.

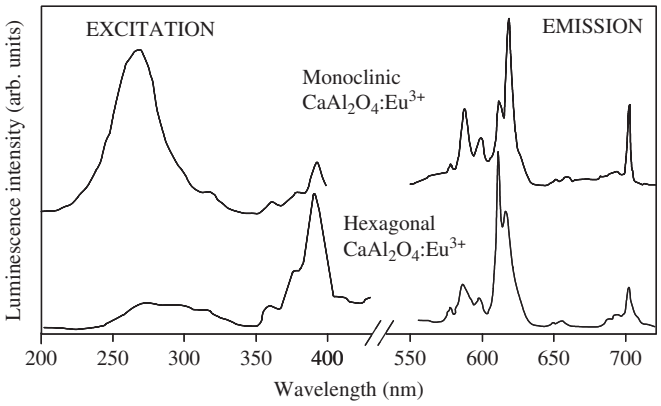

Fig. 4. Steady-state photoluminescence spectra of monoclinic and hexagonal CA : Eu^{3+} at room temperature. Emission was recorded at $\lambda_{exc} = 300$ nm and excitation at $\lambda_{em} = 613$ nm.

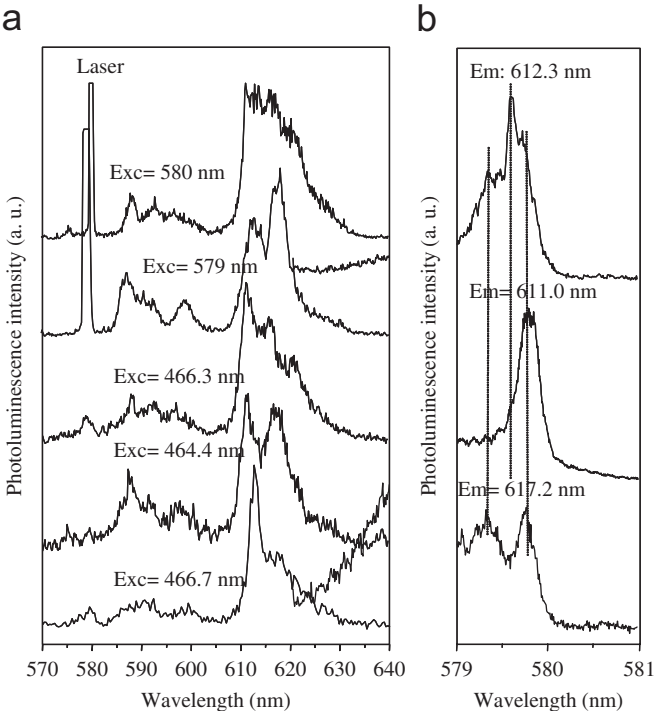

Fig. 5. Site selective emission (a) and excitation (b) spectra of hexagonal CA : Eu^{3+} at 120 K. Delay-time: 200 μs for all the spectra.

possess different chemical environments in the structure. Moreover, the emission lines are relatively broad and unresolved, indicating multiple sites occupancy for the emitting ions. The fact that the $^5D_0 \rightarrow {}^7F_2$ transitions are dominating in the spectra indicates further that the crystallographic sites occupied by Eu^{3+} ions have no inversion symmetry while the observation of a triplet for $^5D_0 \rightarrow {}^7F_1$ transitions reveals that the point site symmetry of Eu^{3+} ions is orthorhombic or lower. The analysis of the excitation spectra in the range corresponding to $^7F_0 \rightarrow {}^5D_0$ transition, which is not splitted by the crystal field, reveals the presence of at least three different crystallographic sites for the Eu^{3+} ions in hexagonal CA : Eu^{3+} (see Fig. 5(b)), in agreement with three independent Ca positions in the structure.

4. Conclusion

Monoclinic and hexagonal undoped and Eu^{3+}-doped calcium aluminate phases were prepared selectively using a sol–gel procedure. Compared to the conventional stable monoclinic phases, the metastable hexagonal phases show specific features in X-ray diffraction, infrared, Raman and photoluminescence spectroscopies which are correlated with the structure of these phases. Especially, it is worth noting that the red Eu^{3+} luminescence is excited preferentially through $O^{2-} \rightarrow Eu^{3+}$ charge transfer mechanism in the case of monoclinic CA : Eu^{3+} while it is excited mainly by direct excitation of the 4f levels in hexagonal CA : Eu^{3+}.

Structural investigation on the metastable phase has allowed to propose an average hexagonal $P6_3$ model, although Rietveld refinement results and spectroscopic study suggest that the real symmetry of the metastable phase is lower. Further structural investigations have to be performed to solve definitively the metastable CA structure and to understand its intriguing spectroscopic behaviour.

Acknowledgements

The authors acknowledge the ERASMUS mobility program for supporting the six months internship period of S. Janáková in the Laboratoire des Matériaux Inorganiques. The authors are also grateful to J. Cellier for technical assistance with X-ray diffraction experiments.

References

[1] Y. Murayama, in: S. Shionoya, W.M. Yen (Eds.), Phosphor Handbook, CRC Press, Boca Raton, FL, USA, 1999, p. 651.
[2] T. Aitasalo, J. Holsa, H. Jungner, M. Lastusaari, J. Niittykoski, J. Lumin. 94–95 (2001) 59.
[3] T. Aitasalo, A. Durygin, J. Holsa, M. Lastusaari, J. Niittykoski, A. Suchocki, J. Alloys Compd. 380 (2004) 4.
[4] J. Holsa, T. Aitasalo, H. Jungner, M. Lastusaari, J. Niittykoski, G. Spano, J. Alloys Compd. 374 (2004) 56.
[5] P.N.M. Dos Anjos, E.C. Pereira, Y.G. Gobato, J. Alloys Compd. 391 (2005) 277.
[6] T. Aitasalo, J. Holsa, H. Jungner, M. Lastusaari, J. Niittykoski, J. Alloys Compd. 341 (2002) 76.
[7] T. Aitasalo, J. Holsa, H. Jungner, M. Lastusaari, J. Niittykoski, M. Parkkinen, R. Valtonen, Opt. Mater. 26 (2004) 113.
[8] J. Rodriguez-Carvajal, Program FullProf 2k, Version 3.40, Laboratoire Léon Brillouin CEA-CNRS, France, 2006.
[9] W. Horkner, H.K. Muller-Buschbaum, J. Inorg. Nucl. Chem. 38 (1976) 983.
[10] S. Ito, K. Ikai, K. Suzuki, M. Inagaki, J. Am. Ceram. Soc. 58 (1975) 79.
[11] A. Altomare, R. Caliandro, M. Camalli, C. Cuocci, C. Giacovazzo, A.G.G. Moliterni, R. Rizzi, Program Expo2004, Version 2.1, Italy, (2006).
[12] V. Favre-Nicolin, R. Cerny, Program Fox, Version 1.6.99CVS (2006), see J. Appl. Cryst. 35 (2002) 734 and Z. Kristallographie 219 (2004) 219.
[13] P. McMillan, B. Piriou, J. Non-Cryst. Solids 55 (1983) 221.
[14] D. Jia, X.-J. Wang, W.M. Yen, Chem. Phys. Lett. 363 (2002) 241.
[15] P. Dorenbos, J. Lumin. 91 (2000) 91.